Targeting the endocannabinoid system in the treatment of fragile X syndrome

Arnau Busquets-Garcia[1], Maria Gomis-González[1], Thomas Guegan[1], Carmen Agustín-Pavón[2,3,11], Antoni Pastor[4,5], Susana Mato[6–8], Alberto Pérez-Samartín[6–8], Carlos Matute[6–8], Rafael de la Torre[1,4,9], Mara Dierssen[2,3,10], Rafael Maldonado[1] & Andrés Ozaita[1]

© 2013 Nature America, Inc. All rights reserved.

Fragile X syndrome (FXS), the most common monogenic cause of inherited intellectual disability and autism[1], is caused by the silencing of the *FMR1* gene, leading to the loss of fragile X mental retardation protein (FMRP)[2], a synaptically expressed RNA-binding protein regulating translation[3]. The *Fmr1* knockout model recapitulates the main traits of the disease[4]. Uncontrolled activity of metabotropic glutamate receptor 5 (mGluR5)[5,6] and mammalian target of rapamycin (mTOR) signaling[7–9] seem crucial in the pathophysiology of this disease. The endocannabinoid system (ECS) is a key modulator of synaptic plasticity, cognitive performance, anxiety, nociception and seizure susceptibility[10], all of which are affected in FXS. The ECS receptors, CB1 (CB1R) and CB2 (CB2R), are activated by phospholipid-derived endocannabinoids. Synaptic activation of mGluR5 initiates the synthesis of endocannabinoids[10,11] and promotes CB1R-driven long-term depression of synaptic strength[10]. Notably, mGluR5 activation is altered in several brain areas of *Fmr1* knockout mice[12–14]. We found that CB1R blockade in male *Fmr1* knockout (*Fmr1*$^{-/y}$) mice through pharmacological and genetic approaches normalized cognitive impairment, nociceptive desensitization, susceptibility to audiogenic seizures, overactivated mTOR signaling and altered spine morphology, whereas pharmacological blockade of CB2R normalized anxiolytic-like behavior. Some of these traits were also reversed by pharmacological inhibition of mTOR or mGluR5. Thus, blockade of ECS is a potential therapeutic approach to normalize specific alterations in FXS.

FXS, the principal monogenic syndrome leading to inherited intellectual disability and autism[15], is caused by an unstable expansion of CGG repeats in the 5′ untranslated region of the gene *FMR1*, producing loss of expression of FMRP (ref. 2). Different factors, including uncontrolled activity of group I metabotropic glutamate receptors, mainly mGluR5[5,6], reduced GABAergic transmission[16,17] and enhanced mTOR signaling[7], seem to have causal roles in FXS deficits.

Synaptic activation of mGluR5 promotes the synthesis of endocannabinoids[11], triggering CB1R-mediated long-term depression (LTD) of excitatory and inhibitory transmission[10]. Notably, deregulated mGluR5-driven LTD has been recently described in several brain areas of adult *Fmr1*$^{-/y}$ mice[12–14]. At the molecular level, ECS activation enhances the phosphatidylinositol-3-kinase (PI3K)–protein kinase B (Akt)-mTOR–p70S6 kinase (p70S6K) signaling pathway in the hippocampus[18,19]. This transduction pathway is closely related to synaptic plasticity[20], is deregulated in *Fmr1*$^{-/y}$ mice[7] and mediates particular behavioral effects of cannabinoids[21], but its pharmacological inhibition has not previously been tested in *Fmr1* knockout mice. Because the ECS has a putative regulatory capacity on most FXS traits, such as cognition, anxiety-like behavior, antinociception and neuronal plasticity[10], we sought to characterize the ECS-mTOR pathway as a potential target for therapeutic intervention in FXS.

We found that acute administration of the CB1R antagonist rimonabant in *Fmr1*$^{-/y}$ mice during the consolidation phase of the object-recognition memory test ameliorated their cognitive deficit without affecting the performance of wild-type (WT) littermates (**Fig. 1a**) or total exploration time (**Supplementary Fig. 1**). Under similar conditions, acute blockade of CB2R with AM630 or of mGluR5 with MTEP were not effective (**Fig. 1b**,**c**). Notably, acute administration of the specific mTOR inhibitor temsirolimus prevented memory impairment (**Fig. 1d**).

When chronically administered, rimonabant, MTEP and temsirolimus, but not AM630, were equally effective at preventing the cognitive deficit in *Fmr1*$^{-/y}$ mice (**Fig. 1e**–**h**). Notably, acute intrahippocampal microinjection of rimonabant during object-recognition memory consolidation improved the cognitive deficit in *Fmr1*$^{-/y}$ mice (**Fig. 1i** and **Supplementary Fig. 2**), pointing to the crucial role of CB1R activity in this brain region in the memory deficit. We next

[1]Departament de Ciències Experimentals i de la Salut (DCEXS), Universitat Pompeu Fabra (UPF), Barcelona, Spain. [2]Centre for Genomic Regulation (CRG), Barcelona, Spain. [3]Universitat Pompeu Fabra (UPF), Barcelona, Spain. [4]Grup de Recerca Clínica en Farmacologia Humana i Neurociències, Institut Hospital del Mar d'Investigacions Mèdiques (IMIM), Barcelona, Spain. [5]Facultat de Medicina, Universitat Autònoma de Barcelona (UAB), Barcelona, Spain. [6]Laboratorio de Neurobiología, Departamento de Neurociencias, Universidad del País Vasco/Euskal Herriko Unibertsitatea (UPV/EHU), Leioa, Spain. [7]Achucarro Basque Center for Neuroscience, Zamudio, Spain. [8]Instituto de Salud Carlos III (ISCIII), Centro de Investigación Biomédica en Red de Enfermedades Neurodegenerativas (CIBERNED), Leioa, Spain. [9]CIBER de Fisiopatología de la Obesidad y Nutrición (CB06/03) (CIBEROBN), Hospital Clínico Universitario Santiago de Compostela, Santiago de Compostela, Spain. [10]CIBER de Enfermedades Raras (CIBERER), Barcelona, Spain. [11]Present address: EMBL-CRG Systems Biology Research Unit, Centre for Genomic Regulation (CRG), Barcelona, Spain. Correspondence should be addressed to A.O. (andres.ozaita@upf.edu).

Received 14 May 2012; accepted 12 February 2013; published online 31 March 2013; doi:10.1038/nm.3127

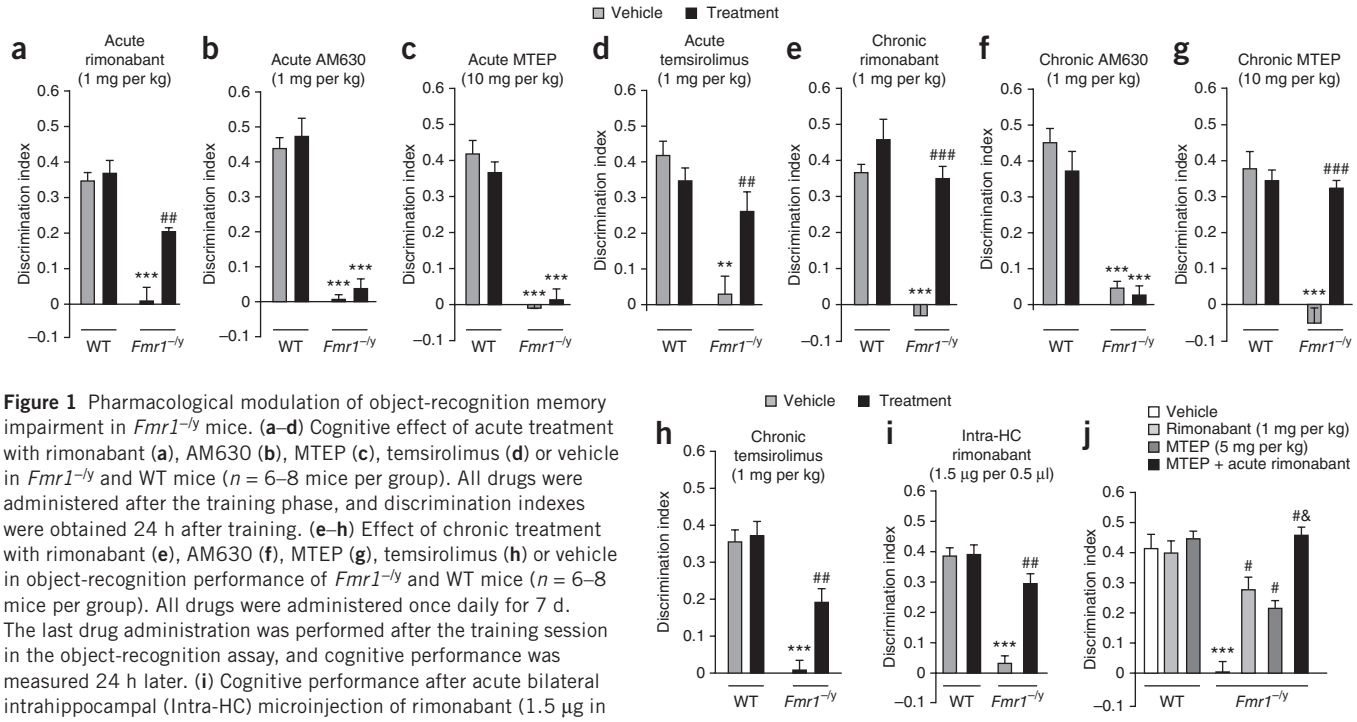

Figure 1 Pharmacological modulation of object-recognition memory impairment in *Fmr1*$^{-/y}$ mice. (**a**–**d**) Cognitive effect of acute treatment with rimonabant (**a**), AM630 (**b**), MTEP (**c**), temsirolimus (**d**) or vehicle in *Fmr1*$^{-/y}$ and WT mice (n = 6–8 mice per group). All drugs were administered after the training phase, and discrimination indexes were obtained 24 h after training. (**e**–**h**) Effect of chronic treatment with rimonabant (**e**), AM630 (**f**), MTEP (**g**), temsirolimus (**h**) or vehicle in object-recognition performance of *Fmr1*$^{-/y}$ and WT mice (n = 6–8 mice per group). All drugs were administered once daily for 7 d. The last drug administration was performed after the training session in the object-recognition assay, and cognitive performance was measured 24 h later. (**i**) Cognitive performance after acute bilateral intrahippocampal (Intra-HC) microinjection of rimonabant (1.5 µg in 0.5 µl per side) or vehicle after the training session. The discrimination index values were obtained 24 h after training and intrahippocampal drug delivery. (**j**) The effect of repeated administration of a suboptimal dose of MTEP combined with an acute administration of rimonabant (see also **Supplementary Fig. 1**). Data are shown as the mean ± s.e.m. $^{***}P < 0.001$, $^{**}P < 0.01$ (*Fmr1*$^{-/y}$ compared to WT); $^{\#}P < 0.05$, $^{\#\#}P < 0.01$, $^{\#\#\#}P < 0.001$ (rimonabant or temsirolimus compared to vehicle); $^{\&}P < 0.05$ (chronic MTEP compared to chronic MTEP + acute rimonabant). Statistical significance was calculated by two-way analysis of variance (ANOVA) with Dunnett's *post hoc* test (**a**–**i**), or one-way ANOVA with Dunnett's *post hoc* test (**j**).

© 2013 Nature America, Inc. All rights reserved.

tested whether mGluR5 and CB1R inhibition converge to normalize the cognitive deficit. MTEP has a short half-life[6] and was only effective after chronic administration. Therefore, we treated mice chronically with a suboptimal dose of MTEP (5 mg per kg body weight) and administered an acute dose of rimonabant after the training session. We found that mice that received the combined treatment had enhanced performance compared with those that received both treatments separately (**Fig. 1j**), pointing to a complementary involvement of both mechanisms.

Recent studies have proposed that Fmrp loss affects the efficacy of mGluR5-driven endocannabinoid production machinery in different brain areas[12–14]. Under our experimental conditions, we did not detect differences between WT and *Fmr1*$^{-/y}$ mice in brain basal amounts of the two main endocannabinoids, 2-arachidonoylglycerol (WT, 100.0% ± 5.7% (mean ± s.e.m.); *Fmr1*$^{-/y}$, 109.7% (as compared to WT) ± 4.8%; $P = 0.213$) and anandamide (WT, 100% ± 4.9%; *Fmr1*$^{-/y}$, 107.4% ± 3.0%; $P = 0.223$), or in the hippocampal expression of several components of the ECS (**Supplementary Fig. 3**), in agreement with previous studies[12,13]. We next examined CB1R-dependent modulation of GABAergic transmission in the hippocampus CA1 area. To estimate possible differences in synaptic endocannabinoid tone, we analyzed the effect of pharmacological CB1R blockade on baseline inhibitory postsynaptic currents (IPSCs) in hippocampal slices from WT and *Fmr1*$^{-/y}$ mice[22]. Bath application of rimonabant increased IPSC amplitude to a similar extent in WT and *Fmr1*$^{-/y}$ mice (**Supplementary Fig. 4a**), suggesting that Fmrp loss does not affect the amount of tonic CB1R activation at GABAergic synapses. Moreover, inhibitory LTD (i-LTD) initiated by mGluR1 and mGluR5 (ref. 10), a form of synaptic plasticity mediated by endocannabinoids, was similarly induced by high-frequency stimulation (HFS) and theta-burst stimulation (TBS) in both WT and *Fmr1*$^{-/y}$ mice (**Fig. 2a**,**b**). Consistently, we detected no differences between WT and *Fmr1*$^{-/y}$ mice in the magnitude of i-LTD elicited by bath application of the mGluR1 and mGluR5 agonist DHPG or in the ability of the CB1R agonist CP55,940 to inhibit GABAergic transmission onto CA1 neurons (**Supplementary Fig. 4**). All of these data suggest that Fmrp removal does not substantially affect the ECS modulation of inhibitory transmission and long-term synaptic plasticity in the hippocampal CA1 area.

The hippocampus of *Fmr1*$^{-/y}$ mice showed a marked increase in the phosphorylation of p70S6K (Thr389) (**Fig. 2c**) that localized to CA1 pyramidal neurons but not GABAergic interneurons (**Fig. 2d**). Remarkably, the phosphorylation status of p70S6K (Thr389) and Akt (Ser473), both of which are involved in mTOR pathway signaling, was specifically enhanced in the hippocampus of *Fmr1*$^{-/y}$ mice (**Fig. 2e** and **Supplementary Fig. 5**). Chronic treatment with either rimonabant or MTEP normalized the phosphorylation of Akt (Ser473) and p70S6K (Thr389) (**Fig. 2e**) in hippocampal tissue. Moreover, as observed in patients with FXS[1], *Fmr1*$^{-/y}$ mice showed an enhanced dendritic spine density of CA1 pyramidal neurons that was also normalized by chronic rimonabant treatment (**Fig. 2f**). When we classified spines on the basis of their morphology, rimonabant-treated *Fmr1*$^{-/y}$ mice showed a decrease in thin and stubby (immature) spines and an increase in mushroom and wide (mature) spines compared to vehicle-treated *Fmr1*$^{-/y}$ mice (**Fig. 2g**), similar to other normalizing interventions[6,9].

Chronic treatment with MTEP or rimonabant normalized both the cognitive deficit and the hippocampal mTOR signaling pathway in adult *Fmr1*$^{-/y}$ mice and showed an additive effect when both treatments were combined, revealing the importance of ECS tone and

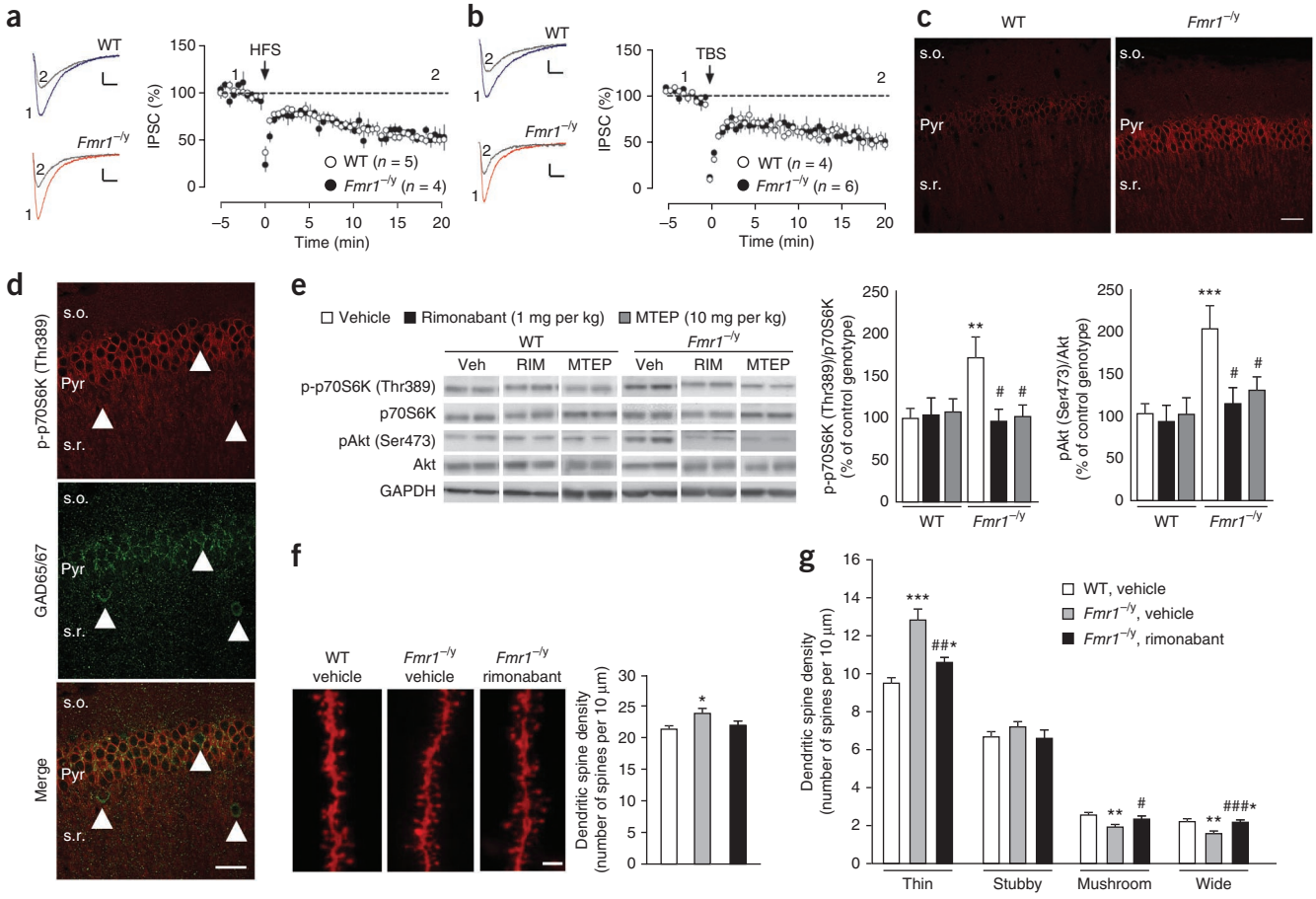

Figure 2 Cellular and molecular effects of pharmacological treatment in adult *Fmr1*$^{-/y}$ mice. (**a**,**b**) Sample traces of IPSCs and average time courses of i-LTD induced by HFS (**a**) and TBS (**b**) in CA1 pyramidal cells of WT and *Fmr1*$^{-/y}$ mice. Traces obtained at time points 1 and 2 are superimposed. Calibration bar, 100 pA, 50 ms. (**c**) Immunofluorescence detection of phosphorylated p70S6K (p-p70S6K) (Thr389) in the CA1 hippocampal region of *Fmr1*$^{-/y}$ and WT mice. Pyr, stratum pyramidale; s.r., stratum radiatum; s.o., stratum oriens. Scale bar, 45 µm. (**d**) Immunodetection of p-p70S6K (Thr389) and 65-kDa or 67-kDa glutamic acid decarboxylase (GAD65/67) (GABAergic neurons, arrowheads) in *Fmr1*$^{-/y}$ mice. Scale bar, 50 µm. (**e**) Phosphorylation of p70S6K (Thr389) and Akt (pAkt) (Ser473) in hippocampal samples from WT and *Fmr1*$^{-/y}$ mice ($n = 6$ mice per group). Data are shown as the mean ± s.e.m. $^{**}P < 0.01$, $^{***}P < 0.001$ (*Fmr1*$^{-/y}$ compared to WT); $^{\#}P < 0.05$ (treatment compared to vehicle). Statistical significance was calculated by two-tailed *t* test. Veh, vehicle; RIM, rimonabant; GAPDH, glyceraldehyde-3-phosphate dehydrogenase. (**f**) Representative DiOlistics staining of hippocampal dendrites in the CA1 field of the hippocampus and overall dendritic spine counts after pharmacological treatments. Scale bar, 2 µm. Data are shown as the mean ± s.e.m. $^{*}P < 0.05$ (*Fmr1*$^{-/y}$ compared to WT) calculated by one-way ANOVA with Dunnett's *post hoc* test. (**g**) Morphological analysis of dendritic spines in the CA1 field of the hippocampus after pharmacological treatments. Data are shown as the mean ± s.e.m. $^{*}P < 0.05$, $^{**}P < 0.01$, $^{***}P < 0.001$ (*Fmr1*$^{-/y}$ compared to WT); $^{\#}P < 0.05$, $^{\#\#}P < 0.01$, $^{\#\#\#}P < 0.001$ (rimonabant compared to vehicle). Statistical significance was calculated by one-way ANOVA with Dunnett's *post hoc* test.

mTOR activity in this cognitive deficit. mTOR signaling is crucial in memory consolidation[23], and genetic regulation of this signaling pathway in *Fmr1*$^{-/y}$ mice prevents some of the *Fmr1*$^{-/y}$ features[9], such as the elevated phosphorylation of translational control molecules, exaggerated protein synthesis, enhanced mGluR-dependent LTD, weight gain, macro-orchidism, immature dendritic spine morphology and behavioral phenotypes, including social interaction deficits, impaired novel object recognition and behavioral inflexibility. We previously showed that mTOR overactivation in CA1 pyramidal neurons is directly involved in the cognitive deficit induced by ECS activation[18,19,21], which can explain the efficacy of rimonabant-mediated CB1R blockade in reversing cognitive impairment in *Fmr1*$^{-/y}$ mice. The fact that temsirolimus also prevented the object-recognition memory deficit in *Fmr1*$^{-/y}$ mice reinforces the concept that overactivation of mTOR signaling has a key role in this deficiency[24] and demonstrates the possibility of using these pharmacological approaches as therapy for this disease. Given that CA1 hippocampal GABAergic presynaptic membranes show 10- to 20-fold higher expression of CB1R than do glutamatergic presynaptic membranes[25], rimonabant might help normalize the balance between excitatory and inhibitory input, which is altered in FXS, and lead to an improved output in the cognitive test by facilitating inhibitory transmission onto CA1 pyramidal cells[26] (**Supplementary Fig. 4**). The balancing effect of rimonabant may also fit with the effect of other therapeutic approaches that aim to re-establish the excitatory-inhibitory balance, such as the mGluR5 antagonist CTEP[6] or the *N*-methyl-D-aspartate (NMDA) receptor antagonist memantine[27], both of which reduce the excitatory drive, and the $GABA_B$ receptor agonist arbaclofen[17], which increases the inhibitory drive.

Adult *Fmr1*$^{-/y}$ mice show a reduced-anxiety phenotype in the elevated plus maze (**Fig. 3a–d** and **Supplementary Fig. 6**) that is reminiscent of the alterations in anxiety observed in patients with FXS[15]. This trait was insensitive to rimonabant or temsirolimus (**Fig. 3a**,**d**).

© 2013 Nature America, Inc. All rights reserved.

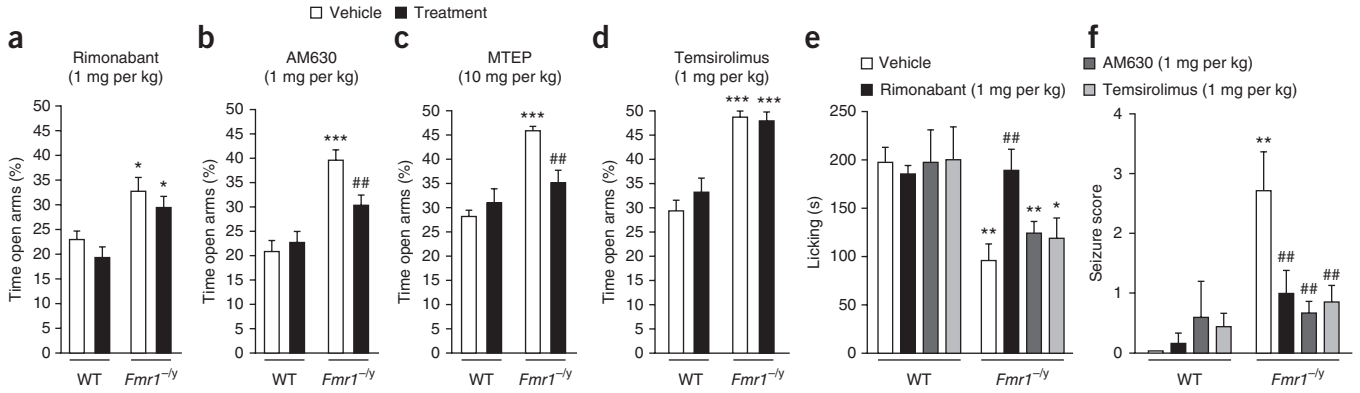

Figure 3 Prevention of other FXS-related phenotypes by pharmacological treatment. (**a**) Anxiety-like behavior in the elevated plus-maze test of WT and *Fmr1*$^{-/y}$ mice (n = 10–12 mice per group) after receiving rimonabant (see also **Supplementary Fig. 6**). (**b**) Anxiety-like behavior in the elevated plus-maze test of WT and *Fmr1*$^{-/y}$ mice (n = 10–12 mice per group) after receiving MTEP. (**c**) Anxiety-like behavior in the elevated plus-maze test of WT and *Fmr1*$^{-/y}$ mice (n = 10–12 mice per group) after receiving AM630. (**d**) Anxiety-like behavior in the elevated plus-maze test of WT and *Fmr1*$^{-/y}$ mice (n = 10–12 mice per group) after receiving temsirolimus. (**e**) Secondary nociceptive response to inflammatory pain of WT and *Fmr1*$^{-/y}$ mice (n = 12–14 mice per group) after receiving rimonabant, AM630 or temsirolimus. (**f**) Audiogenic seizure susceptibility of WT and *Fmr1*$^{-/y}$ mice (n = 6–8 mice per group) after receiving rimonabant, AM630 or temsirolimus. Data (**a**–**f**) are shown as the mean ± s.e.m. $^{*}P < 0.05$, $^{**}P < 0.01$, $^{***}P < 0.001$ (*Fmr1*$^{-/y}$ compared to WT); $^{\#\#}P < 0.01$ (treatment compared to vehicle). Statistical significance was calculated by two-way ANOVA with Dunnett's *post hoc* test.

However, acute CB2R and mGluR5 blockade (**Fig. 3b**,**c**) normalized this phenotype without modifying anxiety-like behavior in WT mice (**Fig. 3b**,**c**). In this regard, CB2R has been involved in the anxiolytic-like effects produced by an enhanced amount of 2-arachidonoylglycerol[18], whereas CB1R has been associated with the anxiolytic-like effect of anandamide accumulation[18]. Because we used doses of rimonabant and AM630 that did not affect the anxiety-like behavior in WT mice, we conclude that the reduced-anxiety phenotype in *Fmr1*$^{-/y}$ mice may specifically involve CB2R signaling.

We used the formalin test to study another characteristic of adult *Fmr1*$^{-/y}$ mice: diminished responses to inflammatory pain, which are sensitive to mGluR5 blockade[28]. This phenotype could be relevant to the self-injurious behavior that is often present in patients with FXS and was only normalized by rimonabant (**Fig. 3e**), consistent with previous findings reported in a different model of peripheral and central nociceptive sensitization[29].

In addition, the marked sensitivity to audiogenic seizures in *Fmr1*$^{-/y}$ mice[30], evoking the enhanced susceptibility of patients with FXS to epilepsy[5], was bluntly decreased by pretreatment with rimonabant, AM630 or temsirolimus (**Fig. 3f**), consistent with results previously reported using mGluR5 antagonism[6]. The involvement of CB2R and mTOR signaling in this phenotypic characteristic reveals a new central effect of these targets.

To further support the contribution of CB1R signaling in behavioral and biochemical manifestations of FXS, we generated a double-mutant *Fmr1* knockout line with a reduced expression of CB1R (*Cnr1*$^{+/-}$). We found that rimonabant-sensitive features in *Fmr1*$^{-/y}$ mice, such as the cognitive deficit (**Fig. 4a** and **Supplementary Fig. 7**), nociceptive desensitization (**Fig. 4b**), audiogenic seizure susceptibility (**Fig. 4c**) and overactivation of the mTOR signaling pathway (**Fig. 4d**), were blunted by the genetic decrease in CB1R expression.

Taken together, our results reveal the involvement of the ECS in specific behavioral, synaptic and molecular manifestations of FXS. We demonstrate that pharmacological or genetic blockade of CB1R normalizes some traits of FXS, such as cognitive impairment, decreased nociceptive response, increased susceptibility to audiogenic seizures and overactivation of the mTOR pathway in the hippocampus. Moreover, CB2R has an important role in the regulation of

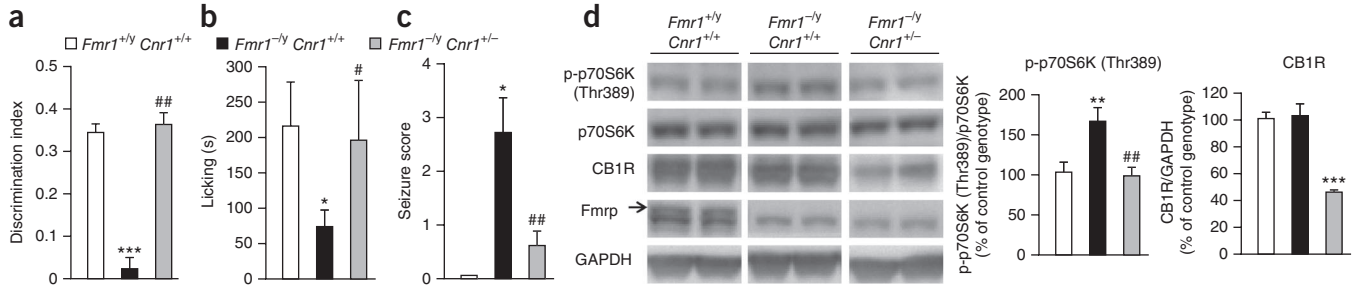

Figure 4 Genetic attenuation of CB1R corrects behavioral deficits and mTOR overactivation in *Fmr1*$^{-/y}$ mice. (**a**) Discrimination index values in the object-recognition test of *Fmr1*$^{+/y}$ *Cnr1*$^{+/+}$ (WT) mice, *Fmr1*$^{-/y}$ *Cnr1*$^{+/+}$ (*Fmr1*$^{-/y}$) and *Fmr1*$^{-/y}$ *Cnr1*$^{+/-}$ mice (n = 6–10 mice per group). (**b**) Secondary nociceptive response to inflammatory pain in WT, *Fmr1*$^{-/y}$ and *Fmr1*$^{-/y}$ *Cnr1*$^{+/-}$ mice (n = 6–10 mice per group). (**c**) Audiogenic seizure susceptibility of WT, *Fmr1*$^{-/y}$ and *Fmr1*$^{-/y}$ *Cnr1*$^{+/-}$ mice (n = 6–10 mice per group). (**d**) p-p70S6K (Thr389), p70S6K, CB1R, Fmrp and GAPDH in hippocampal samples from WT, *Fmr1*$^{-/y}$ and *Fmr1*$^{-/y}$ *Cnr1*$^{+/-}$ mice (n = 6–10 mice per group). The arrow indicates Fmrp detection, distinguished from the nonspecific detection of an extra band with lower molecular weight than Fmrp. Data (**a**–**d**) are shown as the mean ± s.e.m. $^{*}P < 0.05$, $^{**}P < 0.01$, $^{***}P < 0.001$ (*Fmr1*$^{-/y}$ compared to WT); $^{\#}P < 0.05$, $^{\#\#}P < 0.01$ (*Fmr1*$^{-/y}$ *Cnr1*$^{+/-}$ compared to *Fmr1*$^{-/y}$). Statistical significance was calculated by one-way ANOVA with Dunnett's *post hoc* test (**a**–**c**) or two-tailed t test (**d**).

© 2013 Nature America, Inc. All rights reserved.

anxiolytic-like behavior and increased susceptibility to audiogenic seizures. In conclusion, our data point to regulation of the ECS and mTOR pathway as a potential target for the development of new therapeutic approaches in FXS (**Supplementary Fig. 8**).

METHODS

Methods and any associated references are available in the online version of the paper.

Note: Supplementary information is available in the online version of the paper.

ACKNOWLEDGMENTS

We thank C. Fernández-Avilés, D. Real, M. Linares and H. Gómez for expert technical assistance and O.J. Manzoni for helpful comments. *Fmr1* knockout mice in the C57BL/6J background were kindly provided by D. Nelson at Baylor College of Medicine. A.B.-G. is the recipient of a predoctoral fellowship (Ministerio de Educación y Cultura). S.M. is the recipient of a Ramón y Cajal contract (Ministerio de Educación y Cultura). This study was supported by grants from Fundació La Marató de TV3 (090910 to A.O.), Grants from the Ministerio de Ciencia e Innovación (SAF2009-07309 and BFU2012-33500 to A.O., SAF2011-29864 to R.M. and SAF2010-21547 to C.M.), CureFXS E-Rare EU/FIS PS09102673 to M.D., Instituto de Salud Carlos III (RD06/0001/0001 to R.M.), PLAN E (Plan Español para el Estímulo de la Economía y el Empleo), Generalitat de Catalunya (SGR-2009-00731 to R.M. and SGR-2009-00718 to R.d.l.T.) and ICREA (Institució Catalana de Recerca i Estudis Avançats) Academia to R.M.

AUTHOR CONTRIBUTIONS

A.B.-G. participated in experimental design, conducted biochemical and behavioral experiments, and wrote the manuscript. M.G.-G. conducted biochemical and behavioral experiments. T.G. performed dendritic spine morphology analysis. C.A.-P. performed stereotaxic surgeries, and M.D. provided *Fmr1* knockout and WT mice, and discussed the experiments. A.P. and R.d.l.T. measured endocannabinoid levels. S.M. designed and conducted electrophysiological experiments, and wrote the manuscript. A.P.-S. and S.M. were in charge of electrophysiological equipment. C.M. funded the project. R.M. funded the project, participated in experimental design and wrote the manuscript. A.O. conceptualized, participated in experimental design, supervised, funded the project and wrote the manuscript.

COMPETING FINANCIAL INTERESTS

The authors declare no competing financial interests.

Reprints and permissions information is available online at http://www.nature.com/reprints/index.html.

1. de Vries, B.B., Halley, D.J., Oostra, B.A. & Niermeijer, M.F. The fragile X syndrome. *J. Med. Genet.* **35**, 579–589 (1998).
2. Verkerk, A.J. *et al.* Identification of a gene (FMR-1) containing a CGG repeat coincident with a breakpoint cluster region exhibiting length variation in fragile X syndrome. *Cell* **65**, 905–914 (1991).
3. Darnell, J.C. *et al.* FMRP stalls ribosomal translocation on mRNAs linked to synaptic function and autism. *Cell* **146**, 247–261 (2011).
4. Bakker, C.E. *et al.* Fmr1 knockout mice: a model to study fragile X mental retardation. The Dutch-Belgian Fragile X Consortium. *Cell* **78**, 23–33 (1994).
5. Bear, M.F., Huber, K.M. & Warren, S.T. The mGluR theory of fragile X mental retardation. *Trends Neurosci.* **27**, 370–377 (2004).
6. Michalon, A. *et al.* Chronic pharmacological mGlu5 inhibition corrects fragile X in adult mice. *Neuron* **74**, 49–56 (2012).
7. Sharma, A. *et al.* Dysregulation of mTOR signaling in fragile X syndrome. *J. Neurosci.* **30**, 694–702 (2010).
8. Hoeffer, C.A. *et al.* Altered mTOR signaling and enhanced CYFIP2 expression levels in subjects with fragile X syndrome. *Genes Brain Behav.* **11**, 332–341 (2012).
9. Bhattacharya, A. *et al.* Genetic removal of p70 S6 kinase 1 corrects molecular, synaptic, and behavioral phenotypes in fragile X syndrome mice. *Neuron* **76**, 325–337 (2012).
10. Kano, M. *et al.* Endocannabinoid-mediated control of synaptic transmission. *Physiol. Rev.* **89**, 309–380 (2009).
11. Varma, N., Carlson, G.C., Ledent, C. & Alger, B.E. Metabotropic glutamate receptors drive the endocannabinoid system in hippocampus. *J. Neurosci.* **21**, RC188 (2001).
12. Zhang, L. & Alger, B.E. Enhanced endocannabinoid signaling elevates neuronal excitability in fragile X syndrome. *J. Neurosci.* **30**, 5724–5729 (2010).
13. Maccarrone, M. *et al.* Abnormal mGlu 5 receptor/endocannabinoid coupling in mice lacking FMRP and BC1 RNA. *Neuropsychopharmacology* **35**, 1500–1509 (2010).
14. Jung, K.M. *et al.* Uncoupling of the endocannabinoid signalling complex in a mouse model of fragile X syndrome. *Nat. Commun.* **3**, 1080 (2012).
15. Penagarikano, O., Mulle, J.G. & Warren, S.T. The pathophysiology of fragile x syndrome. *Annu. Rev. Genomics Hum. Genet.* **8**, 109–129 (2007).
16. D'Hulst, C. & Kooy, R.F. The GABAA receptor: a novel target for treatment of fragile X? *Trends Neurosci.* **30**, 425–431 (2007).
17. Henderson, C. *et al.* Reversal of disease-related pathologies in the fragile X mouse model by selective activation of $GABA_B$ receptors with arbaclofen. *Sci. Transl. Med.* **4**, 152ra128 (2012).
18. Busquets-Garcia, A. *et al.* Differential role of anandamide and 2-arachidonoylglycerol in memory and anxiety-like responses. *Biol. Psychiatry* **70**, 479–486 (2011).
19. Puighermanal, E., Busquets-Garcia, A., Maldonado, R. & Ozaita, A. Cellular and intracellular mechanisms involved in the cognitive impairment of cannabinoids. *Phil. Trans. R. Soc. Lond. B* **367**, 3254–3263 (2012).
20. Hoeffer, C.A. & Klann, E. mTOR signaling: at the crossroads of plasticity, memory and disease. *Trends Neurosci.* **33**, 67–75 (2010).
21. Puighermanal, E. *et al.* Cannabinoid modulation of hippocampal long-term memory is mediated by mTOR signaling. *Nat. Neurosci.* **12**, 1152–1158 (2009).
22. Lafourcade, M. *et al.* Nutritional omega-3 deficiency abolishes endocannabinoid-mediated neuronal functions. *Nat. Neurosci.* **14**, 345–350 (2011).
23. Richter, J.D. & Klann, E. Making synaptic plasticity and memory last: mechanisms of translational regulation. *Genes Dev.* **23**, 1–11 (2009).
24. Troca-Marín, J.A., Alves-Sampaio, A. & Montesinos, M.L. Deregulated mTOR-mediated translation in intellectual disability. *Prog. Neurobiol.* **96**, 268–282 (2012).
25. Kawamura, Y. *et al.* The CB1 cannabinoid receptor is the major cannabinoid receptor at excitatory presynaptic sites in the hippocampus and cerebellum. *J. Neurosci.* **26**, 2991–3001 (2006).
26. Kang-Park, M.H. *et al.* Differential sensitivity of GABA A receptor–mediated IPSCs to cannabinoids in hippocampal slices from adolescent and adult rats. *J. Neurophysiol.* **98**, 1223–1230 (2007).
27. Wei, H. *et al.* The therapeutic effect of memantine through the stimulation of synapse formation and dendritic spine maturation in autism and fragile X syndrome. *PLoS ONE* **7**, e36981 (2012).
28. Price, T.J. *et al.* Decreased nociceptive sensitization in mice lacking the fragile X mental retardation protein: role of mGluR1/5 and mTOR. *J. Neurosci.* **27**, 13958–13967 (2007).
29. Guindon, J. & Hohmann, A.G. The endocannabinoid system and pain. *CNS Neurol. Disord. Drug Targets* **8**, 403–421 (2009).
30. Chen, L. & Toth, M. Fragile X mice develop sensory hyperreactivity to auditory stimuli. *Neuroscience* **103**, 1043–1050 (2001).

© 2013 Nature America, Inc. All rights reserved.

ONLINE METHODS

Animals. *Fmr1* knockout mice in a FVB background (FVB.129P2-*Pde6b*$^{+}$ *Tyr*$^{c-ch}$*Fmr1*^{tm1Cgr}/J) and WT mice (FVB.129P2-*Pde6b*$^{+}$ *Tyr*$^{c-ch}$/AntJ) were purchased from The Jackson Laboratory and crossed to obtain *Fmr1*$^{-/y}$ and WT littermates. *Fmr1* knockout mice in a C57BL/6J congenic background (B6.129P2-*Fmr1*^{tm1Cgr}/J)[4] were obtained from the Baylor College of Medicine Mouse Facility. Double-mutant mice (*Fmr1*$^{-/y}$ *Cnr1*$^{+/-}$) in a C57BL/6J background were initially generated by crossing homozygous female mice carrying the *Fmr1* mutation (*Fmr1*$^{-/-}$) with homozygous male mice carrying the *Cnr1* mutation (*Cnr1*$^{-/-}$). Subsequently, mice used for experimentation were derived from the crossing of female *Fmr1*$^{+/-}$ *Cnr1*$^{+/+}$ mice with male *Fmr1*$^{+/y}$ *Cnr1*$^{+/-}$ mice. All experimental mice were bred in house at the Barcelona Biomedical Research Park (PRBB) Animal Facility. *Fmr1*$^{-/y}$ and WT mice were used at 12–16 weeks of age, except for in the study of audiogenic seizure susceptibility (where mice were 21–23 d old). Mice were housed four per cage in a temperature-controlled (21 °C ± 1 °C) (mean ± range) and humidity-controlled (55% ± 10%) environment. Food and water were available *ad libitum*. All the experiments were performed during the light phase of a 12 h light, 12 h dark cycle (lights on at 8 a.m. and off at 8 p.m.). Mice were handled for 1 week before starting the experiments. Only male mice were used. All animal procedures followed standard ethical guidelines (European Communities Directive 86/60-EEC) and were approved by the local ethical committee (Comitè Ètic d'Experimentació Animal-Parc de Recerca Biomèdica de Barcelona, CEEA-PRBB). The PRBB also has Animal Welfare Assurance (#A5388-01, Institutional Animal Care and Use Committee approval date 06/08/2009) granted by the Office of Laboratory Animal Welfare (OLAW) of the US National Institutes of Health. All behavioral tests were performed by researchers blind to the different experimental groups.

Drugs and treatments. Rimonabant was obtained from Sanofi-Aventis (Sanofi-Aventis Recherche); AM630 (6-iodo-2-methyl-1-[2-(4-morpholinyl)ethyl]-1H-indol-3-yl](4-methoxyphenyl)methanone), D-APV (DL-2-amino-5-phosphonopentanoic acid), NBQX (2,3-dioxo-6-nitro-1,2,3,4-tetrahydrobenzo[f]quinoxaline-7-sulfonamide disodium salt) and DHPG ((S)-3,5-dihydroxyphenylglycine) were from Tocris Bioscience; MTEP (3-((2-methyl-4-thiazolyl)ethynyl)pyridine) was a kind gift from Merck Research Laboratories; and temsirolimus (CCI-779) was from LC Laboratories. CP55,940 and picrotoxin were purchased from Sigma-Aldrich. Rimonabant, AM630 and MTEP were diluted in 5% ethanol, 5% Cremophor EL and 90% saline. Temsirolimus was dissolved in 2% ethanol, 8% Cremophor EL and 90% saline[31]. All compounds injected intraperitoneally were administered in a volume of 10 ml per kg body weight.

Intrahippocampal administration of rimonabant. Rimonabant (1.5 µg per 0.5 µl) was administered directly into the hippocampus as described elsewhere[32]. After recovery (8 d), mice were administered rimonabant or vehicle bilaterally after the training session in the object-recognition test. After completion of the experimental sequence, cannula position was verified histologically (**Supplementary Fig. 2**), as described previously[32].

Endocannabinoid quantification. Endocannabinoids, 2-AG (2-arachidonoylglycerol) and AEA (anandamide) were analyzed as described previously[18] using half of the right or left brain (including the forebrain, midbrain and hindbrain) (~220–250 mg). The endogenous concentrations of 2-AG and AEA were calculated on the basis of the response of the deuterated analogs and expressed as percentage of control WT mice.

Immunoblot analysis. Tissues from different brain regions (hippocampus, frontal cortex, striatum, amygdala and cerebellum) from WT and *Fmr1*$^{-/y}$ mice were analyzed in basal conditions. Hippocampal tissues from WT and *Fmr1*$^{-/y}$ mice after chronic pharmacological treatment or from the double-mutant mouse line (*Fmr1*$^{+/y}$ *Cnr1*$^{+/+}$, *Fmr1*$^{-/y}$ *Cnr1*$^{+/+}$ and *Fmr1*$^{-/y}$ *Cnr1*$^{+/-}$) were also analyzed. Tissues were processed as previously described[21]. The antibodies used for immunoblotting detected: Fmrp (ab17722, 1:500), monoacylglycerol lipase (MAGL) (ab24701, 1:1,000), fatty acid amide hydrolase (FAAH) (ab54615, 1:500), (Abcam); p-p70S6K (Thr389) (9234, 1:800), p70S6K (9202, 1:500), pAkt (Ser473) (4051, 1:200), Akt (9272, 1:2,000) (all from Cell Signaling Technology); diacylglycerol lipase α (DGL-α) (GP-Af380-1, 1:400), N-acyl phosphatidylethanolamine phospholipase D (NAPE-PLD) (GP-Af720-1, 1:1,000), mGluR5 (GP-Af270-1, 1:1,000), CB1R (Rb-Af380-1, 1:1,000) (all from Frontier Science); and GAPDH (sc-32233, 1:5,000) (Santa Cruz Biotechnology). Optical densities of relevant immunoreactive bands were quantified after acquisition on a ChemiDoc XRS System (Bio-Rad) controlled by The Quantity One software v 4.6.3 (Bio-Rad).

Immunofluorescence. Tissue was prepared as described previously[21]. Hippocampi-containing slices were rinsed in 0.1 M phosphate buffer, incubated in permeabilizing and blocking solution (0.2% Triton X-100, 5% BSA in phosphate buffer) for 2 h and then incubated overnight at 4 °C with antibody to p-p70S6K (Thr389) (9206, 1:100, mouse, Cell Signaling Technology) and antibody to GAD65/67 (AB1511, 1:100, rabbit, Millipore). The next day, after rinsing in phosphate buffer, sections were incubated with antibody to mouse Alexa Fluor 647 (115-165-146, 1:500, Invitrogen) or antibody to rabbit Cy3 (111-225-144, 1:500, Jackson ImmunoResearch Laboratories). After rising, slices were mounted onto gelatin-coated slides with Mowiol mounting medium. Confocal images were obtained as previously described[21].

Slice preparation and electrophysiology. *Fmr1*$^{-/y}$ and WT mice were anesthetized with isoflurane, and their brains were removed to a chilled sucrose-based solution (in mM: 215 sucrose, 2.5 KCl, 26 $NaHCO_3$, 1.6 NaH_2PO_4, 1 $CaCl_2$, 4 $MgCl_2$, 4 $MgSO_4$, 20 glucose and 1.3 mM ascorbic acid), and coronal brain slices (350 µm thick) were cut with a Vibratome Series 3000 Plus-Tissue Sectioning System (Ted Pella, Inc). Sections containing the hippocampus were stored for 30 min at 30–32 °C in recovery solution (in mM: 62 NaCl, 2.5 KCl, 25 $NaHCO_3$, 1.4 NaH_2PO_4, 1.1 $CaCl_2$, 3.3 $MgCl_2$, 2 $MgSO_4$, 15 glucose and 108 sucrose) and then moved into room-temperature low-calcium artificial cerebrospinal fluid (ACSF) (in mM: 124 NaCl, 2.5 KCl, 25 $NaHCO_3$, 1.2 NaH_2PO_4, 1.25 $CaCl_2$, 2.6 $MgCl_2$ and 10 glucose) for at least 1 h. Experiments were conducted at room temperature in a submersion-type recording chamber perfused at 1.5 ml per min with ACSF (same as the low-calcium ACSF with the following exception: 2.5 mM $CaCl_2$ and 1.3 mM $MgCl_2$). All solutions were saturated with 95% O_2 and 5% CO_2, pH 7.4.

Whole-cell recordings were made on visualized CA1 pyramidal neurons voltage clamped at −70 mV with a pipette (2–4 MΩ) containing (in mM): 90 $CsCH_3SO_3$, 50 CsCl, 10 4-(2-hydroxyethyl)-1-piperazineethanesulfonic acid (HEPES), 1 $MgCl_2$, 0.2 ethylene glycol tetraacetic acid (EGTA), 4 Mg^{2+}-ATP, 0.3 Tris-GTP, 5 QX314, pH 7.25, and 285 mOsm). IPSCs were isolated by adding NMDA and α-amino-3-hydroxy-5-methyl-4-isoxazole propionate/kainate (AMPA/KA) receptor antagonists (25 µM D-AP5 and 10 µM NBQX) to the ACSF. To evoke monosynaptic currents, stimuli of duration 150 µs were delivered every 30 s through a patch pipette filled with ACSF and placed in the stratum radiatum. Series resistance (typically 10–20 MΩ) was monitored through the experiments by applying a −2 mV hyperpolarizing pulse before each evoked IPSC, and cells with a more than 20% change in this parameter were excluded from the analysis. LTD was induced by HFS (2 trains of 100 pulses at 100 Hz 20 s apart) or TBS (10 bursts of 5 stimuli applied at 100 Hz with 200 ms interburst intervals repeated 4 times 5 s apart). The magnitude of LTD and the effects of the different drugs were estimated by comparing averaged responses corresponding to the last 5 min of the experiment with baseline-averaged responses 5 min before the induction protocol or the beginning of drug application. Recordings were performed with a MultiClamp 700B (Axon Instruments), and output signals were filtered at 3 kHz. Data were digitized (10 kHz) on a DigiData 1332A (Axon Instruments). Data were collected using Clampex 9.2, and IPSC amplitude was analyzed using Clampfit 9.2.

Dendritic spine morphology analysis. Dendritic spine analysis was performed as previously described[33] in mice that received chronic administration of rimonabant (1 mg per kg body weight for 7 d) or vehicle. Brains were extracted after perfusion (4% paraformaldehyde (PFA) in phosphate buffer) 3 h after the last administration of rimonabant or vehicle solution on the seventh day of treatment. Secondary to tertiary dendrites of pyramidal neurons

© 2013 Nature America, Inc. All rights reserved.

doi:10.1038/nm.3127

from the CA1 region of the hippocampus were chosen for spine analysis on the basis of criteria described previously[33].

Object-recognition task. Object-recognition memory was assayed as described previously[21]. All acute treatments and the last administration of the chronic treatments were performed after the training session in the object-recognition test.

Anxiety-like response. Anxiety-like responses were evaluated as previously described[18]. Briefly, 5-min test sessions were performed 120 min after drug administration. The time spent in the open arms as well as the total number of entries in the arms were recorded.

Nociceptive response. The late-phase nociceptive response (corresponding to inflammatory pain)[34] was recorded during 20 min starting 20 min after formalin (5%, 20 µl) injection into the right hind paw. All drugs were injected 20 min before the formalin injection. The nociceptive behavior (licking) was measured.

Audiogenic seizure sensitivity. Mice were placed individually into an observation chamber, a glass cylinder 40 cm high and 16 cm in diameter, and allowed to explore for 1 min. Next, a bell (100 dB) rung for 30 s. Mice were tested only once. Seizure activity was scored as follows: no response, 0; wild running, 1; clonic seizure, 2; tonic seizure, 3; status epilepticus, respiratory arrest or death, 4. Drugs were administered 30 min before the test.

Statistical analyses. Results are reported as the mean ± s.e.m. Most of the experiments were evaluated by one-way analysis of variance (ANOVA) followed by Dunnett's *post-hoc* test when required. Two-way ANOVA (rimonabant, AM630, MTEP, temsirolimus treatment versus WT or *Fmr1*$^{-/y}$ genotype) was used when required. Statistical comparisons of electrophysiological data were performed using Student's *t* test. Comparisons were considered statistically significant when $P < 0.05$.

31. Puighermanal, E. *et al.* Dissociation of the pharmacological effects of THC by mTOR blockade. *Neuropsychopharmacology* advance online publication, http://dx.doi.org/10.1038/npp.2013.31 (2013).
32. Castañé, A., Maldonado, R. & Valverde, O. Role of different brain structures in the behavioural expression of WIN 55,212–2 withdrawal in mice. *Br. J. Pharmacol.* **142**, 1309–1317 (2004).
33. Guegan, T. *et al.* Operant behavior to obtain palatable food modifies neuronal plasticity in the brain reward circuit. *Eur. Neuropsychopharmacol.* **23**, 146–159 (2013).
34. Noble, F. *et al.* Pain-suppressive effects on various nociceptive stimuli (thermal, chemical, electrical and inflammatory) of the first orally active enkephalin-metabolizing enzyme inhibitor RB 120. *Pain* **73**, 383–391 (1997).

© 2013 Nature America, Inc. All rights reserved.